

# INTERNATIONAL SOCIETY FOR SOIL MECHANICS AND GEOTECHNICAL ENGINEERING



*This paper was downloaded from the Online Library of the International Society for Soil Mechanics and Geotechnical Engineering (ISSMGE). The library is available here:*

<https://www.issmge.org/publications/online-library>

*This is an open-access database that archives thousands of papers published under the Auspices of the ISSMGE and maintained by the Innovation and Development Committee of ISSMGE.*

*The paper was published in the proceedings of the 3<sup>rd</sup> International Symposium on Coupled Phenomena in Environmental Geotechnics and was edited by Takeshi Katsumi, Giancarlo Flores and Atsushi Takai. The conference was originally scheduled to be held in Kyoto University in October 2020, but due to the COVID-19 pandemic, it was held online from October 20<sup>th</sup> to October 21<sup>st</sup> 2021.*

## Behavior of hazardous metal(loid)s release from excavated marine sedimentary rock under atmospheric exposure with drying-wetting cycles

Yuto Yoshida <sup>i)</sup>, Hirofumi Sakanakura <sup>ii)</sup>, Toshihiko Miura <sup>iii)</sup> and Masahiko Katoh <sup>iv)</sup>

i) Undergraduate Student, Department of Agricultural Chemistry, Meiji University, 1-1-1, Higashi-mita, Tama, Kawasaki, Kanagawa, 214-8571, Japan.

ii) Head, Center for Material Cycles and Waste Management Research, National Institute for Environmental Studies, 16-2 Onogawa, Tsukuba, Ibaraki, 305-8506, Japan

iii) Vice Minister, Technical Research Institute, Obayashi Corporation, 4-640 Shimo-kiyoto, Kiyose, Tokyo, 204-8558, Japan

iv) Associate Professor, Department of Agricultural Chemistry, Meiji University, 1-1-1, Higashi-mita, Tama, Kawasaki, Kanagawa, 214-8571, Japan.

### ABSTRACT

Large amounts of marine sedimentary rock are excavated for the construction of modern high-speed railways and roads, and they pose environmental risk due to the release of hazardous metal(loid)s. It is therefore important understand how hazardous metal(loid)s are released from excavated rock. This study investigated the influences of alteration surface structure of excavated rock induced by atmospheric exposure with drying-wetting cycles on the release of hazardous metal(loid)s. The atmospheric exposure with the drying-wetting cycles caused the particle size reduction, but not carbonation. In addition, it induced the oxidation of framboidal pyrite, resulting in the increase in the sulfate ion release and decrease in the pH in the excavated rock. The amount of amorphous iron content decreased with the increase in the period of atmospheric exposure. The amounts of arsenic, lead, and fluoride ion release were decreased with the increase in the period of atmospheric exposure, while those of selenium was gradually increased. The amount of boron release was stable during the atmospheric exposure. On the basis of these results, this study suggests that the atmospheric exposure with the drying-wetting cycles enhances/suppresses the release of hazardous metal(loid)s from the excavated rock.

**Keywords:** carbonation, particle size reduction, oxidation, pyrite

### 1 INTRODUCTION

Large amounts of rock and/or sediments are excavated to create underground space for the construction of modern high-speed railways and roads around the world. The excavated rock and/or sediment naturally contains hazardous metal(loid)s at the background level such as arsenic during the sedimentation and hydrothermal metamorphism. In urbanized coastal areas, marine sedimentary rock that frequently contains low levels of framboidal pyrite is excavated. The contents of hazardous metal(loid)s in the excavated marine sedimentary rock are the background levels, but the excavation often alters the hazardous metal(loid) phases to more soluble due to the increase of specific surface area, exposure of water and air, and drying. The excavated marine sedimentary rock becomes an environmental concern if the level of hazardous metal(loid) release exceeds the environmental standard for soil. Thus, it is important to understand how hazardous metal(loid)s are released from the excavated marine sedimentary rock for their reuse without posing environmental risks (Katsumi, 2015).

The excavated marine sedimentary rock is re-used as embankments and roadbed materials. In these

applications, the excavated marine sedimentary rock is exposed to rainfall and outside temperature changes, in particular near the surface. The exposure may cause the repetition of wetting and drying. Furthermore, atmospheric oxygen and carbon dioxide as well as rainwater may promote the oxidation of framboidal pyrite and carbonation in the excavated marine sedimentary rock. These reactions have a potential to alter the surface structure of excavated marine sedimentary rock, resulting in the changes in the release behavior of hazardous metal(loid)s in the excavated marine sedimentary rock. However, it has not been understood that how the behavior of hazardous metal(loid) release is changed with the alteration of surface structure of excavated marine sedimentary rock although arsenic release from the excavated marine sedimentary rock is increased/decreased with the oxidation of framboidal pyrite (Kamata and Katoh, 2019).

This study conducted the test of atmospheric exposure with the drying-wetting cycles using the excavated marine sedimentary rock. The amounts of hazardous metal(loid)s released and magnitude of pyrite oxidation, particle size reduction, and carbonation were investigated to understand the changes in the behavior of

hazardous metal(loid) release with the atmospheric exposure.

## 2 MATERIALS AND METHODS

### 2.1 Preparation of excavated marine sedimentary rock

Excavated marine sedimentary rock samples of 50–70 cm in diameter were collected from tunnel construction sites on the central part of Honshu island, Japan. Rock was excavated from the Kazusa Group at a Pleistocene depth of 50–70 m. To remove oxidized parts of rock samples, 5–10 mm of rock surfaces were scraped off using a stainless steel spoon. Rock samples were then crushed using a chisel, hammer, and an agate mortar, and were then stored at  $-20^{\circ}\text{C}$  to prevent oxidation. The particle size distribution of rock sample was 38% for  $<0.075$  mm, 10% for 0.075–0.106 mm, 26% for 0.106–0.250 mm, 22% for 0.250–0.425 mm, and 3% for  $>0.425$  mm. Table 1 shows the chemical properties of rock samples and Table 2 shows Elemental composition of using X-ray fluorescence Spectrometer (XRF; ZSX Primus IV, Rigaku Co., Japan).

### 2.2 Atmospheric exposure with repetition of increase/decrease of moisture content

Crushed samples were placed on a bat and were kept in the glass greenhouse. During atmospheric exposures, ultra-pure water was added at two or three times a week to maintain at the initial water content ratio of 20 wt% when the moisture content decreased to 5–8 wt%. Temperature and humidity were monitored every hour during the test period using a data logger (Thermo Recorder TR-72wb, T&D Corporation, Japan) (Fig. 1). Moisture content was calculated on the basis of decreased amount of rock sample. The test started on August 9, 2020, and exposed samples were collected at 0, 1, and 3 months.

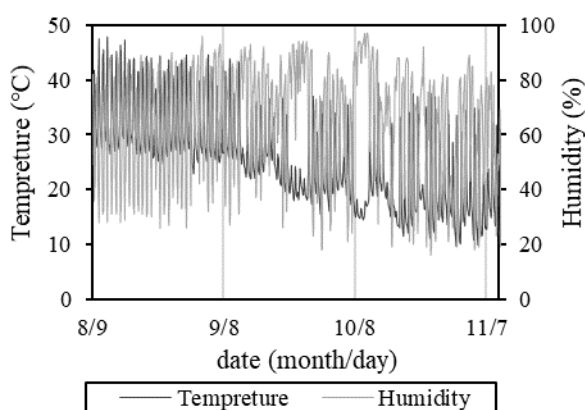


Fig. 1. Temperature and humidity under atmospheric exposure.

Table 1. Chemical properties of excavated marine sedimentary rock samples (based on dried weights).

pH	EC (mS/m)	WS-OC (mg/kg)	Am-Fe (mg/g)	Moisture content ratio (%)	Loss-on-ignition (%)
6.7±0.1	53±1	285±12	5.7±0.1	20.9±0.2	7.8±0.0

WS-OC : Water soluble organic carbon, Am-Fe : Amorphous Iron

Table 2. Elemental composition of excavated marine sedimentary rock samples.

SiO <sub>2</sub> (wt.%)	TiO <sub>2</sub> (wt.%)	Al <sub>2</sub> O <sub>3</sub> (wt.%)	Fe <sub>2</sub> O <sub>3</sub> (wt.%)	MnO (wt.%)	MgO (wt.%)	CaO (wt.%)	Na <sub>2</sub> O (wt.%)	K <sub>2</sub> O (wt.%)	P <sub>2</sub> O <sub>5</sub> (wt.%)
62.20	0.85	18.88	7.12	0.09	2.43	2.77	1.61	2.78	0.10

erature and humidity were monitored every hour during the test period using a data logger (Thermo Recorder TR-72wb, T&D Corporation, Japan) (Fig. 1). Moisture content was calculated on the basis of decreased amount of rock sample. The test started on August 9, 2020, and exposed samples were collected at 0, 1, and 3 months.

### 2.3 Batch leaching test

Batch leaching tests were conducted in 50-ml polypropylene tubes. In these experiments, 30-ml aliquots of ultra-pure water were added to  $3.000 \pm 0.001$ g dry weights of exposed samples so that the *L/S* ratio was 10, and the tubes were shaken on a horizontal shaker at 200 rpm for 24 h. Suspensions were then separated by centrifugation (5000 rpm for 5 min) and filtered through 0.45- $\mu\text{m}$  membrane filters. After the measurement of pH and EC in filtrates using a pH meter, a portion of filtrates was acidified below pH 2 using 1 M HNO<sub>3</sub>. The concentrations of arsenic, selenium, cadmium, and lead in acidified filtrates were determined using graphite furnace atomic absorption spectrometry (Z-3000, Hitachi, Ltd., Japan). The concentrations of boron in acidified filtrates and fluoride and sulfate ions in non-acidified filtrates were determined using inductively coupled plasma optical emission spectrometry (ICP-OES; Optima 8300, PerkinElmer Co., Ltd., USA) and ion chromatography with an INTEGRION system and a Dionex IonPac™ AS22 IC column (Thermo Fisher Scientific Inc., USA), respectively. The amounts of hazardous metal(loid)s released from the exposed sample was calculated on the basis of *L/S* ratios. All experiments were performed in triplicate.

### 2.4 Amorphous iron content

Amorphous iron was extracted using 0.2 M oxalate buffer solution (pH 3.0) according to the method of Shuman (Shuman, 1985). Extract solutions were then passed through 0.45- $\mu\text{m}$  filters for analysis using atomic absorption spectrometry (Z-3000, Hitachi, Ltd., Japan). The amounts of amorphous iron in the exposed sample was calculated on the basis of *L/S* ratios. All experiments were performed in triplicate.

### 2.5 X-ray diffraction analysis and observation with digital microscope of exposed rock

Mineralogical composition analyses were performed

using X-ray diffraction (XRD; MultiFlex, Rigaku Co., Japan) with Cu K $\alpha$  radiation at 40 kV and 40 mA. The XRD data were analyzed using PDXL software (Rigaku Co., Japan) equipped with the ICDD Powder Diffraction File. The exposed rock samples were examined using digital microscope (VHX-7000, Keyence Co., Japan) in order to observe the size distribution of particle.

### 3 RESULTS AND DISCUSSION

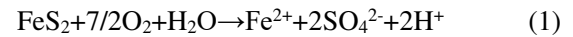
#### 3.1 Moisture content during atmospheric exposure

Figure 2 shows the percentage of moisture content during the atmospheric exposure. The one drying-wetting cycle was defined as the period from the addition of ultra-pure water to the next addition of ultra-pure water. Drying-wetting of 23 and 56 cycles were conducted for 1- and 3-months atmospheric exposure.

#### 3.2 pH, EC, and sulfate ion release in excavated rock with atmospheric exposure

The pH values of excavated rock decreased with the increase in the period of atmospheric exposure (Fig. 3). In contrast, the EC values increased with the increase in the period of atmospheric exposure (Fig. 4). The amount of sulfate ion released from the excavated rock was also increased with the increase in the period of atmospheric exposure (Fig. 5). The sample used in this study contains framboidal pyrite. (Kamata and Katoh, 2019). The decrease

in pH value and increase in the sulfate ion release would result from the oxidation of framboidal pyrite in the excavated rock with the atmospheric oxygen and water by the following reaction:



The increase in the sulfate ion release would mainly contribute to the increase in the EC value.

#### 3.3 Amorphous iron content during atmospheric exposure

The amount of amorphous iron in the excavated rock gradually decreased with the increase in the period of atmospheric exposure (Fig. 6). Oxalate buffer solution extracts iron hydroxide from the sample as Amorphous iron. The oxidation of pyrite causes the formation of iron hydroxides (Kimura et al., 1999). Thus, it has been expected the increase in the amount of amorphous iron with the increase in the period of atmospheric exposure. However, the amount of amorphous iron was decreased. The crystalline structure of iron hydroxide precipitated by pyrite oxidation could increase with further aging, making it harder to extract using organic acids such as citric and oxalic acid (Choppala, 2017). Therefore, a decrease in the amount of amorphous iron resulting from an increase in the crystallinity of iron hydroxide could

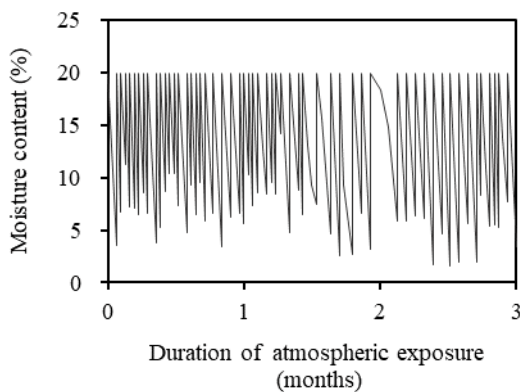


Fig. 2. Moisture content with atmospheric exposure.

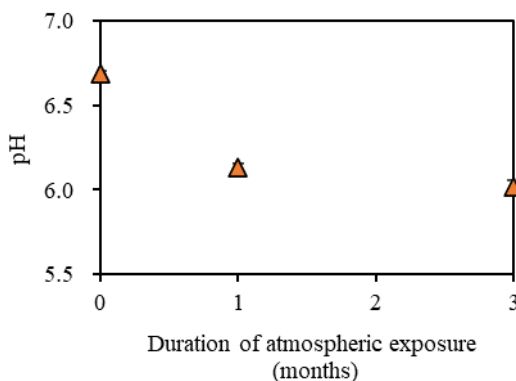


Fig. 3. pH of excavated rock with atmospheric exposure.

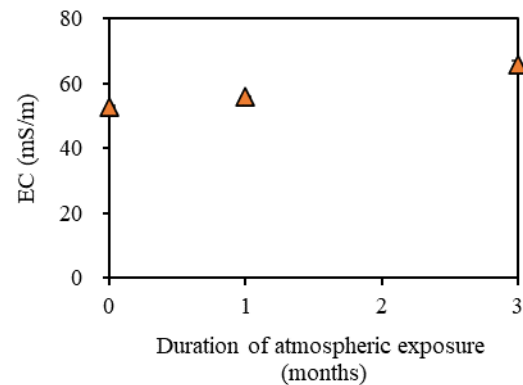


Fig. 4. Electric Conductivity (EC) of excavated rock with atmospheric exposure.

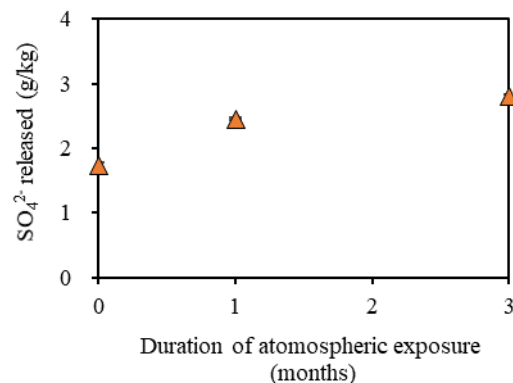


Fig. 5. SO<sub>4</sub><sup>2-</sup> released from excavated rock with atmospheric exposure.

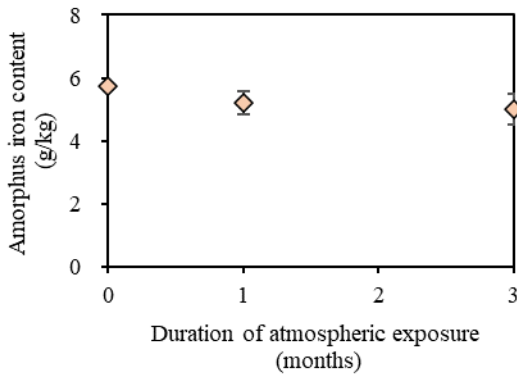


Fig. 6. Amorphous iron in excavated rock with atmospheric exposure.

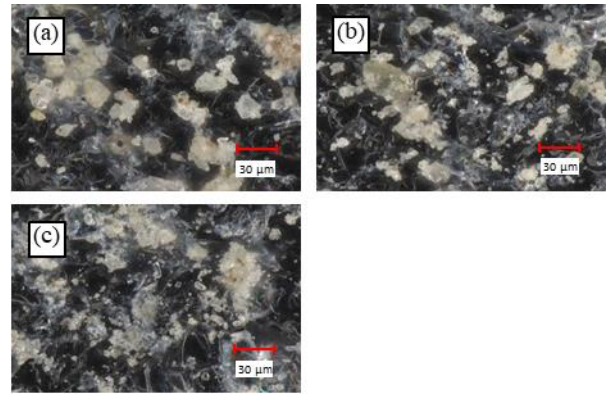


Fig. 8. Digital microscope photomicrographs of excavated rock (a) before and (b) 1-month and (c) 3-month atmospheric exposure.

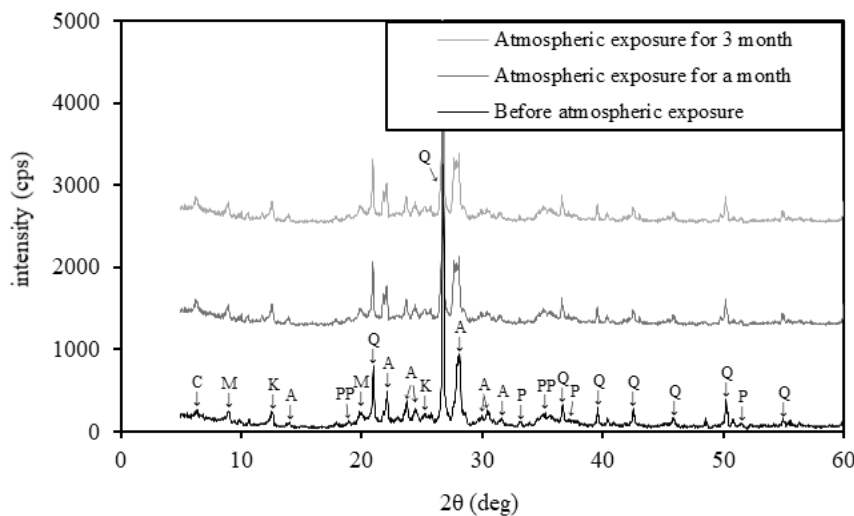


Fig. 7. X-ray diffraction profiles of excavated rock with the atmospheric exposure. Q:Quartz, A:Albite, C:Chlorite, M:Muscovite, K:Kaolinite, PP:Pyrope, P:Pyrite

framboidal pyrite, decreasing the amount of amorphous iron.

### 3.4 Alteration in mineral structure with atmospheric exposure

Figure 7 shows the XRD profiles of excavated rock with the atmospheric exposure. Quartz ( $\text{SiO}_2$ ), albite ( $\text{NaAlSi}_3\text{O}_8$ ), chlorite, muscovite, and kaolinite ( $\text{Al}_2\text{Si}_2\text{O}_5(\text{OH})_4$ ) were identified as the dominant crystalline minerals despite the period of atmospheric exposure. In addition, the trace peaks of pyrope ( $\text{Mg}_3\text{Al}_2(\text{SiO}_4)_2$ ) and pyrite ( $\text{FeS}_2$ ) were also detected from the excavated rock despite the atmospheric exposure. The strengths of XRD peak after the atmospheric exposure were not increased/decreased compared with those before the atmospheric exposure. Moreover, no carbonate minerals were detected from the excavated rocks after any periods of atmospheric exposure.

The digital microscope observation confirmed that most of the particles were larger than 10  $\mu\text{m}$  in diameter

in the excavated rock before the atmospheric exposure (Fig. 8). The number of particles with a diameter of 10–30  $\mu\text{m}$  was decreased, and those of less than 10  $\mu\text{m}$  were found in the excavated rock after the atmospheric exposure. The same observation was found from the 20-sample observation, suggesting that particle size reduction of excavated rock was occurred by the atmospheric exposure.

### 3.5 Hazardous metal(loid) release from excavated rock with atmospheric exposure

The amount of arsenic released decreased from 0.042 mg/kg to 0.018 mg/kg after 1-month atmospheric exposure, and then were stable at 0.018 mg/kg after 3-month atmospheric exposure (Fig. 9). The amount of selenium released was 0.087 mg/kg before the atmospheric exposure. That gradually increased to 0.095 mg/kg after 3-month atmospheric exposure. The amounts of boron released was stable during the atmospheric exposure (Fig. 10). In contrast, the amount of fluoride ion released greatly decreased from 2.4 mg/-

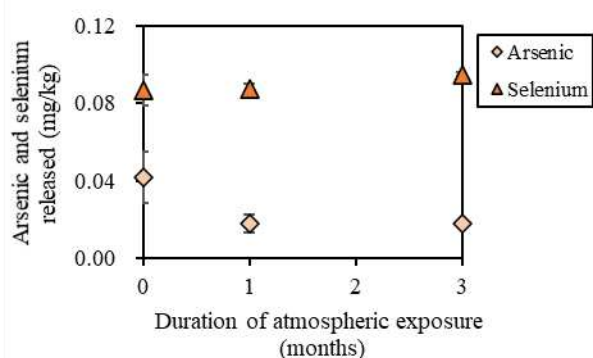


Fig. 9. Arsenic and selenium released from excavated rock with atmospheric exposure.

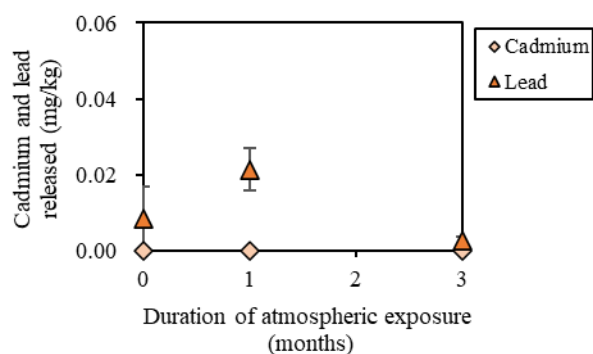


Fig. 10. Boron and fluoride released from excavated rock with atmospheric exposure.

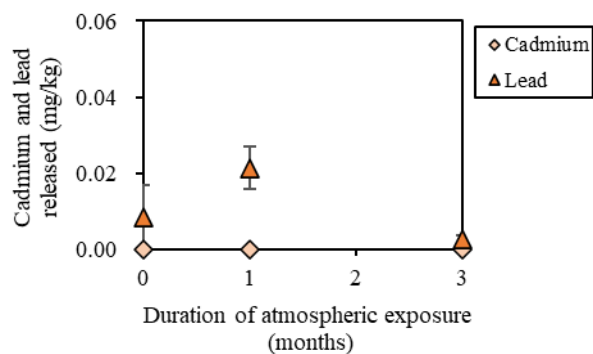


Fig. 11. Cadmium and lead released from excavated rock with atmospheric exposure.

kg to 0.6–0.9 mg/kg after the atmospheric exposure. Cadmium released was not detected from the excavated rock despite the atmospheric exposure, suggesting that low content of cadmium in the excavated rock used in this study (Fig. 11). The amount of lead released temporarily increased, and then decreased with the increase in the period of atmospheric exposure.

### 3.6 Hazardous metal(loid) release from excavated rock with mineral structure changes with atmospheric exposure

In this study, the oxidation of framboidal pyrite, particle size reduction, and carbonation have been expected by the atmospheric exposure with the drying-

wetting cycles. The oxidation of framboidal pyrite was confirmed on the basis of the results of increase in the sulfate ion release and decrease in pH value with the increase in the period of atmospheric exposure while the increase in the amount of amorphous iron was not found. On the basis of observation by the digital microscope, the particle size reduction was induced by the atmospheric exposure. The particle size reduction would lead to the increase in the hazardous metal(loid) release due to the increase in the specific surface area. However, the amounts of hazardous metal(loid)s released was not increased except selenium. This suggests that the increase in the specific surface area by the particle size reduction would not much enhance the hazardous metal(loid)s release from the excavated rock. In addition, the particle size reduction would not change the crystalline structure in the excavated rock due to the no changes of XRD peaks before and after the atmospheric exposure. Carbonation was not also confirmed. These suggest that the oxidation of framboidal pyrite was the main factor to increase/decrease the hazardous metal(loid) release after the atmospheric exposure. The factors to increase their releases would be the oxidation of framboidal pyrite and particle size reduction. In contrast, the factors to decrease their decrease would be the sorption by the iron hydroxide. In the case of arsenic, lead, and fluoride ion, the factors to decrease might exceed the factors to increase, which resulted in the decrease in their releases. However, in the case of selenium, the factors to increase might exceed the factors to decrease, which resulted in the increase in its release. Boron is dissolved as  $B(OH)_3$  under pH of 6 (Kakihana, 1977). In addition, boron would not be released by the oxidation of framboidal pyrite, which would result in the no alteration in the boron release with the increase in the period of atmospheric exposure.

## 4 CONCLUSION

This study investigated the behavior of hazardous metal(loid)s release from the excavated rock with the atmospheric exposure with the drying-wetting cycles. The atmospheric exposure with the drying-wetting cycles caused the particle size reduction, but not carbonation. In addition, it induced the oxidation of framboidal pyrite, resulting in the increase in the sulfate ion release and decrease in the pH in the excavated rock. The amount of amorphous iron content did not increase, but decreased with the increase in the period of atmospheric exposure. The amounts of arsenic, lead, and fluoride ion release were decreased with the increase in the period of atmospheric exposure, while those of selenium was gradually increased. The amount of boron release was stable during the atmospheric exposure. On the basis of these results, this study suggests that the atmospheric exposure with the drying-wetting cycles enhances/suppresses the release of hazardous metal(loid)s from the excavated rock.

## ACKNOWLEDGEMENTS

This study was supported by the Japan Society for the Promotion of Science (JSPS) KAKENHI [grant number 20K12211].

## REFERENCES

- 1) Katsumi, T. (2015): Soil excavation and reclamation in civil engineering: environmental aspect, *Soil Sci Plant Nutr*, 61, 22-29.
- 2) Kamata, A. and Katoh, M. (2019): Arsenic release from marine sedimentary rock after excavation from urbanized coastal areas: Oxidation of framboidal pyrite and subsequent natural suppression of arsenic release, *Science of the Total Environment*, 670, 752-759.
- 3) Shuman, L. M. (1985): Fractionation method for soil microelements, *Soil Science*, 140 (1), 11-22.
- 4) Kimura, S., N, Shikazono., Nohara, M. and Iwai, S. (1999): Behavior of Trace and Rare Earth Elements with Chemical Weathered Sedimentary Rocks, Miocene Onnagawa Formation, Oga Peninsula, *Journal of Japan Society of Engineering Geology*, 40, 5, 281-294.
- 5) Choppala, G., Bush, R., Moon, E., Ward, N., Wang, Z., Bolan, N. and Sullivan, L., (2017): Oxidative transformation of iron monosulfides and pyrite in estuarine sediments: Implications for trace metals mobilization, *Journal of Environmental Management*. 186, 158–166.
- 6) Kakihana, H., Kotaka, M., Satoh, S., Nomura, M. and Okamoto, M. (1977): Fundamental Studies on the Ion-Exchange Separation of Boron Isotopes, *Bulletin of the Chemical Society of Japan*, 50, 1, 158-163.